



# Alpha-synuclein supports type 1 interferon signalling in neurons and brain tissue

Brendan Monogue,<sup>1,2</sup> Yixi Chen,<sup>3,4</sup> Hadrian Sparks,<sup>1</sup> Ranya Behbehani,<sup>3</sup> Andrew Chai,<sup>3</sup> Alexander J. Rajic,<sup>5</sup> Aaron Massey,<sup>2</sup> B. K. Kleinschmidt-Demasters,<sup>5,6</sup> Matthieu Vermeren,<sup>3</sup>  Tilo Kunath<sup>3,4</sup> and  J. David Beckham<sup>1,2,5,7</sup>

The protein alpha-synuclein is predominantly expressed in neurons and is associated with neurodegenerative diseases like Parkinson's disease and dementia with Lewy bodies. However, the normal function of alpha-synuclein in neurons is not clearly defined. We have previously shown that mice lacking alpha-synuclein expression exhibit markedly increased viral growth in the brain, increased mortality and increased neuronal cell death, implicating alpha-synuclein in the neuronal innate immune response.

To investigate the mechanism of alpha-synuclein-induced immune responses to viral infections in the brain, we challenged alpha-synuclein knockout mice and human alpha-synuclein knockout dopaminergic neurons with RNA virus infection and discovered that alpha-synuclein is required for neuronal expression of interferon-stimulated genes. Furthermore, human alpha-synuclein knockout neurons treated with type 1 interferon failed to induce a broad range of interferon stimulated genes, implying that alpha-synuclein interacts with type 1 interferon signalling. We next found that alpha-synuclein accumulates in the nucleus of interferon-treated human neurons after interferon treatment and we demonstrated that interferon-mediated phosphorylation of STAT2 is dependent on alpha-synuclein expression in human neurons. Next, we found that activated STAT2 co-localizes with alpha-synuclein following type 1 interferon stimulation in neurons. Finally, we found that brain tissue from patients with viral encephalitis expresses increased levels of phospho-serine129 alpha-synuclein in neurons.

Taken together, our results show that alpha-synuclein expression supports neuron-specific interferon responses by localizing to the nucleus, supporting STAT2 activation, co-localizing with phosphorylated STAT2 in neurons and supporting expression of interferon-stimulated genes. These data provide a novel mechanism that links interferon activation and alpha-synuclein function in neurons.

- 1 Department of Immunology and Microbiology, University of Colorado Anschutz Medical Campus, Aurora, CO 80045, USA
- 2 Division of Infectious Diseases, Department of Medicine, University of Colorado Anschutz Medical Campus, Aurora, CO 80045, USA
- 3 Centre for Regenerative Medicine and the School of Biological Sciences, University of Edinburgh, Edinburgh EH16 4UU, UK
- 4 UK Centre for Mammalian Synthetic Biology, University of Edinburgh, Edinburgh EH16 4UU, UK
- 5 Department of Neurology, University of Colorado Anschutz Medical Campus, Aurora, CO 80045, USA
- 6 Departments of Pathology and Neurosurgery, University of Colorado Anschutz Medical Campus, Aurora, CO 80045, USA
- 7 Rocky Mountain Regional VA Medical Center, Aurora, CO 80045, USA

Correspondence to: J. David Beckham  
University of Colorado Anschutz Medical Campus  
Building Research 1 North  
12800 East 19th Ave, B8333  
Aurora, CO 80045, USA  
E-mail: david.beckham@cuanschutz.edu

**Keywords:** alpha-synuclein; interferon; neuron; virus; brain

**Abbreviations:**  $\alpha$ Syn = alpha-synuclein; hESC = human embryonic stem cell; IFNR = type 1 interferon receptor; ISG = interferon stimulated gene; MFI = mean fluorescence intensity; T1IFN = type 1 interferon; VEEV = Venezuelan equine encephalitis virus; WNV = West Nile virus

## Introduction

Alpha-synuclein ( $\alpha$ Syn), a 14 kDa protein encoded by the SNCA gene, is best known as the primary component of Lewy bodies found in patients with Parkinson's disease as well as other synucleinopathies.<sup>1</sup>  $\alpha$ Syn is predominately expressed in neurons both in the central and peripheral nervous systems as well as red blood cells.<sup>2,3</sup> Previous studies exploring a functional role for  $\alpha$ Syn expression in neurons have suggested a variety of potential cellular functions. Most notably, studies have suggested a potential role for  $\alpha$ Syn in regulating synaptic transmission and vesicle transport. *Snca*<sup>-/-</sup> mice show an increased release of dopamine with paired stimuli and a corresponding reduction in striatal dopamine levels.<sup>4</sup> Basal dopamine levels were also shown to be reduced in the absence of both alpha-synuclein and beta-synuclein, although not in single gene knockout animals.<sup>5</sup> Additionally,  $\alpha$ Syn-deficient mice have impaired hippocampal synaptic responses to prolonged stimuli that are associated with a deficiency in undocked vesicles in the synapse.<sup>6</sup> This function of  $\alpha$ Syn in regulating synaptic transmission and vesicle transport may be tied to an association between  $\alpha$ Syn and SNARE-proteins.<sup>7</sup> In addition to this potential native function of  $\alpha$ Syn, recent evidence suggests a role for this protein in facilitating innate immune responses in the CNS.

Numerous studies suggest  $\alpha$ Syn modulates innate immune responses in the CNS. We previously reported that  $\alpha$ Syn knockout (KO) mice (*Snca*<sup>-/-</sup>) exhibit increased mortality and disease severity from viral encephalitis, accompanied by increased viral growth in the brain following peripheral challenge with RNA viruses including West Nile virus (WNV) and Venezuelan equine encephalitis virus (VEEV) TC83.<sup>8</sup> A subsequent study demonstrated that total  $\alpha$ Syn expression was elevated in gastrointestinal-associated neurons following viral gastroenteritis in children.<sup>9</sup> The same study also suggested that  $\alpha$ Syn expression supported chemotaxis and activation of infiltrating dendritic cells.<sup>9</sup> A more recent follow-up study has shown that  $\alpha$ Syn is a critical mediator of inflammatory and immune responses in the gastrointestinal tract by supporting T-cell responses.<sup>10</sup>  $\alpha$ Syn was additionally shown to be necessary for controlling intranasal infection with reovirus and intravenous infection with *Salmonella typhimurium*.<sup>11</sup> Another study was able to show that intranasal inoculation of Western equine encephalitis virus resulted in loss of dopaminergic neurons in the substantia nigra and formation of prominent proteinase K-resistant aggregates of phospho-serine129  $\alpha$ Syn (pS129  $\alpha$ Syn).<sup>12</sup> Taken together, these studies have shown that acute infection increases  $\alpha$ Syn expression in mice, increases phosphorylation of  $\alpha$ Syn at serine residue 129 and can result in loss of nigral dopamine neurons; thereby recapitulating multiple key neuropathological features of Parkinson's disease. Despite these important recent findings, the mechanisms underlying the functional role of  $\alpha$ Syn in the CNS immune response remain unclear.

In the current study, we performed RNA-Seq analysis on whole brain tissue from wild-type and  $\alpha$ Syn knockout mice infected with WNV to determine differences in gene expression that may contribute to the deficient immune response in  $\alpha$ Syn knockout mice. We found that  $\alpha$ Syn knockout mice exhibited deficiencies in the expression of several interferon-stimulated genes (ISGs) that are critical for

the control of viral infection in the CNS. To investigate cell types in the brain that may require  $\alpha$ Syn-dependent immune function, we next used human dopaminergic neurons differentiated from wild-type and  $\alpha$ Syn knockout human embryonic stem cells (hESCs).<sup>13</sup> We found that  $\alpha$ Syn knockout neurons challenged with VEEV TC83 exhibited significantly increased viral growth. Following stimulation of human and mouse neurons with type 1 interferon (T1IFN), we next found that  $\alpha$ Syn localizes to the nucleus, co-localizes with phosphorylated STAT2, that STAT2 phosphorylation is dependent on  $\alpha$ Syn expression and that ISG expression is significantly reduced in the absence of  $\alpha$ Syn. In human brain tissue, we also show that patients with WNV encephalitis exhibit increased pS129  $\alpha$ Syn expression in neurons. Thus, our data are the first to demonstrate that  $\alpha$ Syn functions to modulate interferon signalling in human neurons by co-localizing and supporting STAT protein activation to induce a robust ISG responses.

## Materials and methods

### Experimental model and subject details

#### Ethics statement

All animal work was performed at the University of Colorado Anschutz Medical Campus in accordance with and following approval by the Institutional Animal Care and Use Committee. All work with live viruses and recombinant DNA was approved by the University of Colorado Institutional Biosafety Committee and performed in accordance with local and national regulations of pathogens. Human brain tissue was obtained from de-identified human autopsies at the University of Colorado Hospital with approval for non-human research by the local Colorado Multiple Institutional Review Board. All work with hESCs was completed at the University of Edinburgh and ethics approval was granted by the MRC Steering Committee for the UK Stem Cell Bank and for the Use of Stem Cell Lines (ref. SCSC13–19).

#### Cell culture

See the [Supplementary material](#) for details. All cell lines were maintained at 37°C in 5% CO<sub>2</sub>. SNCA<sup>-/-</sup> and SNCA<sup>+/+</sup> hESCs were generated and differentiated towards midbrain dopaminergic neural progenitors to Day 16 by the Kunath laboratory as previously described.<sup>13</sup> Following this, the cells were cryopreserved as described<sup>14</sup> and shipped to the Beckham laboratory. Cells were then thawed and plated in Laminin-111 (BioLamina)-coated 48-well plates at a density of 800 000 cells/cm<sup>2</sup> in neuronal differentiation media consisting of Neurobasal Media (Thermo Fisher Scientific) + B27 supplement (without Vitamin A, 1:50, Thermo Fisher Scientific) + L-glutamine (2 mM, Thermo Fisher Scientific) supplemented with ascorbic acid (0.2 mM, Sigma), brain-derived neurotrophic factor (20 ng/ml, Peprotech), glial cell line-derived neurotrophic factor (10 ng/ml, Peprotech), dibutyryl cyclic AMP (0.5 mM, Sigma) and DAPT (1  $\mu$ M, Tocris). Y27632 (10  $\mu$ M, Tocris) was present in medium from Day 16 to Day 17. Cells were differentiated for an additional 26 days (42 days of total differentiation) and media was replenished every 3–4 days. RC17 hESCs were

differentiated into cortical neurons using a dual-SMAD inhibition protocol.<sup>15</sup> Murine primary cortical neurons were harvested from E18 C57BL/6J embryos as previously described.<sup>16</sup>

### Virus propagation and quantification

See the [Supplementary material](#) for additional details. WNV strain 385–99 (NY99) was obtained from clone derived virus and propagated in *Aedes albopictus* (C6/36, ATCC CRL-1660) cells as previously described.<sup>8</sup> VEEV TC83 isolates were obtained from the laboratory of Dr Michael Diamond at Washington University in St. Louis and was propagated in BHK cells. Viral titres for all viruses were quantified in Vero cells by standard plaque assay as previously described.<sup>8</sup>

### Mouse studies

*Snca*<sup>−/−</sup> mice and wild-type mice were obtained from Jackson Laboratories (#3692) and back-crossed seven generations to C57BL/6J mice (#664). Microsatellite analysis performed by Jackson Laboratories confirmed mice were 96.3% C57BL/6J. These mice were crossed with wild-type C57BL/6J mice to generate *Snca*<sup>+/-</sup> heterozygous mice. Genotyping by conventional PCR was routinely performed to confirm *Snca* status as described.<sup>8</sup> Interferon knockout mice were obtained from Jackson laboratories (#28256).

Prior to subcutaneous inoculation of virus, all mice were randomized, weighed and placed under isoflurane-induced anaesthesia. Equal numbers of male and female mice were used for all studies with the exception of the use of only female mice for the total brain RNAseq analysis. Murine virus infections were completed as previously described.<sup>8</sup> Samples collected for RNA gene expression assays or viral quantification were collected and stored in RNALater (Invitrogen, #AM7021) or PBS, respectively.

### Neuronal cell culture infections and interferon treatments

SNCA<sup>−/−</sup> and SNCA<sup>+/-</sup> hESC-derived midbrain dopaminergic and cortical neurons were grown as described above. Following this, the cellular medium was removed and replaced with complete neuronal differentiation media (described above) containing VEEV TC83 virus at a multiplicity of infection (MOI) of 1. Three hundred microlitres of the media were removed and replaced with fresh, virus-free neuronal differentiation media every 12 h for 72 h. The viral content of these samples was then titred via plaque assay as described previously.<sup>8</sup> Differentiated 15 neurons were infected with VEEV-TC83 at an MOI of 10. Twelve hours post-infection, RNA from these cells was extracted and analysed via qPCR (described below). Differentiated neurons were treated with 10 000 IU/ml of mixed-type human IFN $\alpha$ , 25  $\mu$ g/ml of Poly(I:C), or mock treated. RNA from these cells was extracted 4 h post-treatment and analysed via qPCR and protein studies were completed at the indicated time points.

### RNAseq studies and gene expression assays

See the [Supplementary material](#) for detailed methods. RNAseq analysis was performed on bulk brain RNAs by Novogene. Analysis of sequencing reads completed by Novogene and additional analysis of Fastq files was completed in the Beckham and Kunath laboratories. Following total RNA quantification (Nanodrop) from brain tissue, we completed mRNA enrichment (poly-T oligo-attached magnetic beads), cDNA synthesis, end repair, poly-A and adaptor addition, fragment selection and PCR and library quality assessment (Agilent2100) followed by Illumina sequencing (NovaSeq). Following data clean-up, clean reads representing 96.51% of total reads were available for analysis with approximately 60–80 million reads per sample. Mouse

genome sequence alignment was completed with STAR with 85.7% of reads mapping to exons and fragments per kilobase of transcript sequence per millions base pairs sequenced (FPKM) calculated for gene expression. Qiagen's custom RT<sup>2</sup> Profiler PCR array was used to assay isolated microglia and neurons from infected mouse brain for ISGs and microglia activation markers. RNA extraction and purification, cDNA synthesis, and Qiagen RT<sup>2</sup> custom PCR array was performed according to the manufacturer's protocol and recommendations. Bio-Rad's PrimePCR probe-based qPCR assays for *Oas1b*, *Irf9*, *Tlr3*, *Trim25*, *Tgtp1* and *Mx1* were used to verify RNAseq results.

### Immunocytochemistry

Differentiated hESC-derived neurons and murine primary neurons were grown on Laminin-111 treated coverslips placed inside 24-well plates as described above. Neurons were then treated with IFN $\alpha$ 2 for 1 or 4 h at a concentration of 10 000 IU/ml. Following this, cells were fixed and washed three times with Dulbecco's PBS (D-PBS). Cells were then permeabilized (0.3% Triton-X in D-PBS), blocked in 5% goat serum in D-PBS, and immunostained at 1:300 dilution of mouse anti-human alpha-synuclein antibody conjugated to FITC (Novus), rabbit anti-human pSTAT2 antibody (Invitrogen), pSTAT2 Tyr631 (Thermo Fisher, #105860), pSTAT1 Tyr701 (Cell Signaling Technology, #9167), IFNAR1 (CST, #18015; Thermo Fisher, #82612) or  $\alpha$ Syn (Abcam 190376) overnight at 4°C. Cells were then incubated in a 5% goat serum solution in D-PBS containing a 1:200 dilution of relevant secondary antibody. An Olympus FV1000 confocal laser scanning biological microscope (Olympus) was used for imaging analysis. Human cortical neurons treated and fixed were blocked with 2% goat serum for 30 min, permeabilized with 0.1% Triton X-100 and stained for total  $\alpha$ Syn (BD Biosciences 610787) and beta-III Tubulin (R and D Systems MAB1195) overnight, then stained for secondary antibodies Alexa 488 (Thermo Fisher A21121) and Alexa 568 (Thermo Fisher A21134). Imaging was conducted with Leica SP8 confocal imaging at 63 $\times$  magnification. All images were randomized, blinded and given to a separate researcher for qualitative analysis of co-localization (FIJI Co-loc, Manders analysis scoring). For cortical neurons, images were processed using ImageJ macro (w/StarDist plugin, courtesy of Dr Matthieu Vermeren). Quantified image data was processed using R Studio script with a threshold of 5000 MFI (mean fluorescence intensity) for IFN $\alpha$ 2, 4000 MFI for IFN $\beta$ , and 10  $\mu$ m<sup>2</sup> DAPI-stained area set as a distinguisher of nuclear localization in viable cells, whereby the threshold was used to calculate percentage of nuclear-localized nuclei per image. Analysis and cumulative frequency distribution analysis (PRISM 9) were used to exclude basal level nuclear localization.

### Brain digestion, cell isolation and flow cytometry

Cells collected from adult, infected mouse brain for flow cytometry were obtained as described.<sup>17</sup> The data was acquired on a LSRII flow cytometer (BD) using voltages standardized according to previously published methods.<sup>18</sup> FlowJo software (FlowJo, LLC, Ashland, Oregon) was used to analyse the data. See the [Supplementary material](#) for detailed methods.

### Immunohistochemistry of human tissue

Unstained slides prepared from formalin-fixed, paraffin-embedded tissue were obtained from various brain regions from patient cases at autopsy. Slides from midbrain, basal ganglia, thalamus, pons, frontal



cortex and superior cerebellum were obtained from WNV-positive cases or control cases (Supplementary Table 3). Slides from a patient with Parkinson's disease and increased phospho-S129  $\alpha$ Syn (pS129  $\alpha$ Syn) expression was used as a positive control. Blank slides were de-paraffinized, antigen retrieval was performed via the HIRS method using Vector Antigen Unmasking stock solution diluted 100 $\times$  (Vector), blocked with Blocking Buffer (TSBB, Thermo Scientific), immunostained with antibodies to pS129  $\alpha$ Syn (Abcam EP1536Y), MAP2 (Novus, 1:100) diluted in TSBB at a concentration of 1:300, followed by TRITC-labelled secondary antibodies (1:100) and mounted with VectaMount mounting medium (Vector). Slides were visualized for fluorescence using Olympus FV version 4.2 software on an Olympus confocal microscope 1000. Three regions from each available slide were imaged. Fluorescence scoring was quantified using Fiji. Total area fluorescence mean, area and raw intensity were measures for all slides.

## Quantification and statistical analysis

### Sample sizes

The number of mice ( $n$ ) is provided in the figure legends.

### Statistical analysis

The Shapiro–Wilk test was first applied to test for normality. If normality was met, t-test or one-way ANOVA was used to prepare differences between two or more groups. If normality was not met, the non-parametric Mann–Whitney U-test or Kruskal–Wallis one-way ANOVA was used to prepare differences between two or more groups. For parametric ANOVA tests, the Tukey's honestly significant difference test was used for comparing differences between two groups post ANOVA with equal variances, and the Games–Howell *post hoc* test used with unequal variances. For non-parametric ANOVA tests, the Dunn's test was used to compare between two groups.

## Resource availability

### Lead contact

Further information and requests for reagents may be directed to and be fulfilled by the corresponding author, Dr J. David Beckham (david.beckham@cuanschutz.edu).

### Materials availability

Experimental models (organisms, strains) generated for use in this study will be made available on request, but we may require a completed Materials Transfer Agreement if there is potential for commercial application.

### Data availability

The published article includes all data sets generated or analysed during this study. Groups A, B, C and D represent mock-infected wild-type, mock-infected  $\alpha$ Syn knockout, WNV-infected wild-type and WNV-infected  $\alpha$ Syn knockout mice, respectively. Gene expression data are available at NCBI (Accession GSE205140) or by request.

## Results

### Alpha-synuclein supports immune gene expression in brain tissue

Following our previous work showing increased viral growth and increased mortality in  $\alpha$ Syn knockout mice upon viral infection,<sup>8</sup>

we analysed the transcriptome of wild-type and  $\alpha$ Syn knockout whole mouse brain tissue following infection with WNV [1000 plaque-forming units (pfu), subcutaneous (s.c.) inoculation]. Brains were harvested 8 days post-infection with WNV or mock infection, and RNA-seq was performed to determine differences in the transcription profile of these treatment groups. The mock-infected mice had highly similar profiles (Supplementary Fig. 1), with only four genes having differential gene expression including the *Snc* gene (Fig. 1A), indicating little variation in the gene expression of animals at basal state. Both genotypes of mice exhibited marked alterations in their expression profiles following WNV infection. There were 1317 upregulated genes in wild-type mice following WNV infection and 1785 upregulated genes in  $\alpha$ Syn knockout mice following WNV infection (Fig. 1). In addition, there were 87 downregulated genes in the WNV-infected wild-type mice and 375 downregulated genes in the WNV-infected  $\alpha$ Syn knockout mice (Fig. 1). Notably, we found substantially more upregulated and downregulated genes in the knockout mice compared to the wild-type mice, suggesting greater dysregulation of gene expression in the  $\alpha$ Syn knockout mice. When comparing WNV-infected  $\alpha$ Syn knockout mouse brain tissue to wild-type mice, we found 35 genes with significantly upregulated expression, and 50 genes that were significantly downregulated in the brain tissue of  $\alpha$ Syn knockout mice (Fig. 1). Immune-related genes that are important for antiviral responses were among the most upregulated in both  $\alpha$ Syn knockout and wild-type mice. However, several immune-associated genes showed significant downregulation in  $\alpha$ Syn knockout mice compared to wild-type mice including *Herc6*, *Tnfrsf25* and *Crip3* (Supplementary Table 1). These data together indicate that  $\alpha$ Syn plays a role in gene regulation during infection. We subsequently looked for immune genes that had lower expression in WNV-infected  $\alpha$ Syn knockout mice compared to WNV-infected  $\alpha$ Syn wild-type mice that may explain a potential immune deficiency in the brain tissue that resulted in significantly increased WNV growth in the brain as we have previously shown.<sup>8</sup> We found that *Herc6* (Fig. 1E), *Oas1b* (Fig. 1F) and *Ift2* (Fig. 1G) all showed evidence of decreased gene expression in the brain tissue of WNV-infected  $\alpha$ Syn knockout mice compared to WNV-infected wild-type mice. Given the higher viral loads previously seen in the brain tissue of WNV-infected  $\alpha$ Syn knockout mice compared to WNV-infected wild-type mice,<sup>8</sup> we would expect to see greater expression of these genes in the  $\alpha$ Syn KO mice if  $\alpha$ Syn was not impacting gene expression. These data indicated that  $\alpha$ Syn may have a role in regulation of innate immune gene expression in the brain following viral infection.

We next investigated the expression of ISGs in WNV-infected  $\alpha$ Syn KO and wild-type mice based on prior data showing that ISG expression in the brain is an important factor in WNV infection.<sup>19–22</sup> We infected  $\alpha$ Syn knockout and wild-type mice with WNV (1000 pfu, sc) or mock infection, and we harvested whole brain at 8 days post-infection. Using quantitative reverse transcription (qRT)-PCR analysis we evaluated the expression of five target ISGs that exhibited decreased expression in the RNAseq analysis of WNV-infected  $\alpha$ Syn knockout mice (*Oas1b*, *Irf9*, *Tlr3*, *Trim25* and *Tgtp1*) and one gene that exhibited no significant changes in expression when comparing WNV-infected  $\alpha$ Syn knockout and wild-type mice (*Mx1*) (Fig. 2A–F). We found that WNV-infected  $\alpha$ Syn knockout mice exhibited approximately a 2-fold decrease in expression of *Oas1b*, *Irf9*, *Tlr3* and *Trim25* genes in brain tissue compared wild-type mice (Fig. 2A–D). Similarly, WNV-infected  $\alpha$ Syn knockout mice exhibited a 4-fold decrease in *Tgtp1* gene expression in brain tissue compared to wild-type mice (Fig. 2E). Consistent with our transcriptomic analysis,

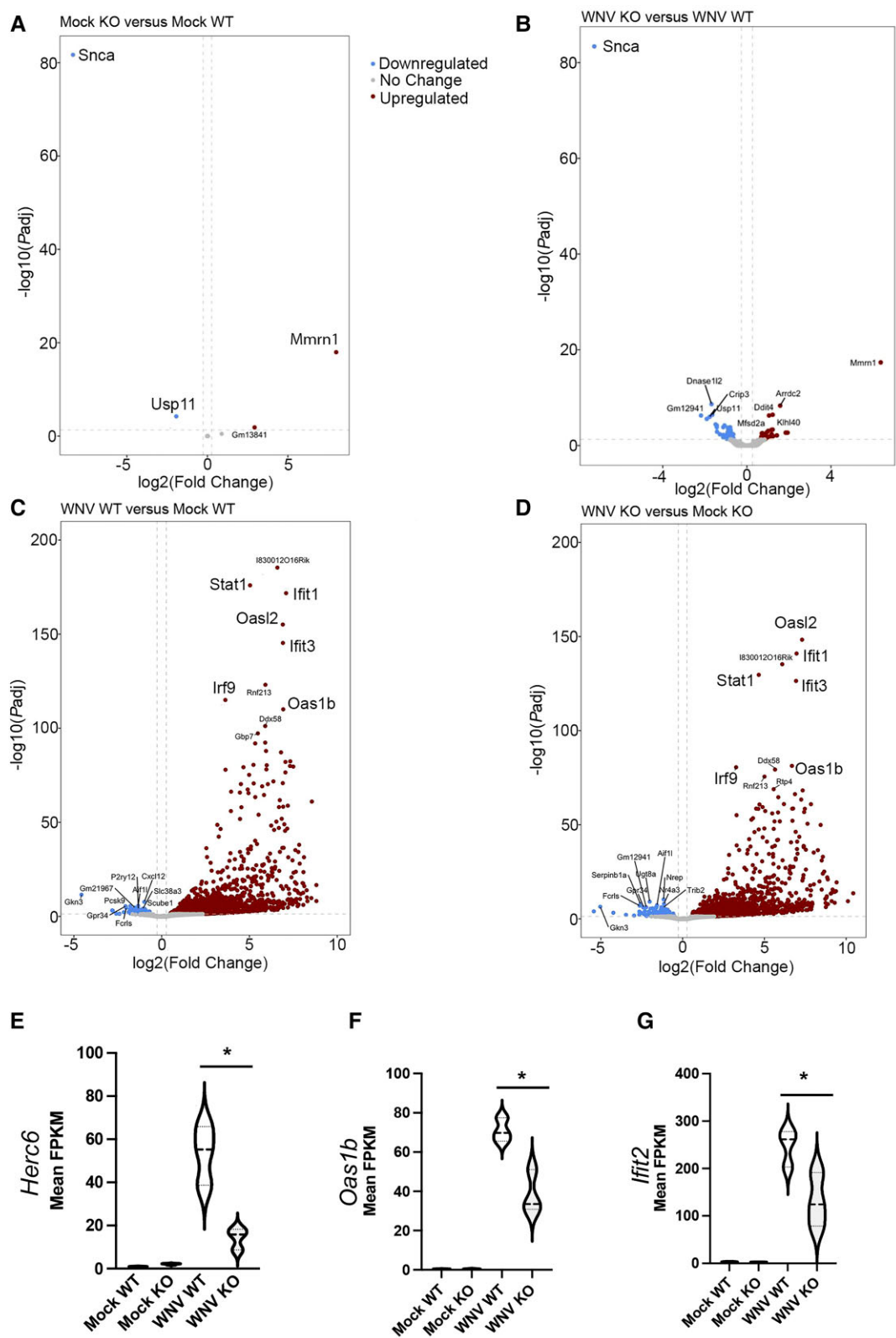


**Figure 1** RNAseq analysis reveals a group of virus-induced genes that are dependent on  $\alpha$ Syn expression in the brain. C57BL6/J mice were treated with mock or WNV (1000 pfu/sc) inoculum and brain tissue harvested at Day 8 post-infection for RNAseq analysis of whole brain tissue. Volcano plots showing comparative gene expression following infection were created comparing (A) mock-infected knockout (KO) compared to mock-infected wild-type (WT) mice, (B) WNV-infected knockout compared to WNV-infected wild-type mice, (C) WNV-infected wild-type compared to mock-infected wild-type mice and (D) WNV-infected knockout compared to mock-infected knockout mice. Mean FPKM values for (E) *Herc6*, (F) *Oas1b* and (G) *Ifit2* are reduced in WNV-infected knockout brain tissue compared to wild-type brain tissue.  $n = 4$  mice/group. WT = wild-type mice; KO =  $\alpha$ Syn knockout mice. \* $P < 0.01$ . ANOVA with Tukey's multiple comparisons.

we found that  $\alpha$ Syn gene expression had no effect on Mx1 gene expression in the brains of WNV-infected  $\alpha$ Syn knockout and WT mice (Fig. 2F). These data supported our initial transcriptomic data showing that  $\alpha$ Syn is required to support the full complement of ISG expression in brain tissue following WNV infection.

### Alpha-synuclein regulates viral growth within neurons

We have previously shown that an attenuated alphavirus, VEEV TC83, exhibits robust infection in the brains of  $\alpha$ Syn knockout mice following peripheral infection while causing no detectable infection in the brains of wild-type mice.<sup>8</sup> Prior studies have shown that VEEV TC83 strain is attenuated in part due to a mutation that reduces viral resistance to Ifit1 restriction, an ISG that recognizes viral RNA and restricts translation.<sup>23</sup> To evaluate intrinsic  $\alpha$ Syn-dependent inhibition of VEEV TC83 in brain tissue, we evaluated VEEV TC83 growth in the brain following intracranial inoculation in wild-type and  $\alpha$ Syn knockout mice. WNV cannot be used in these studies due to high mortality rate in mice and neurons following direct intracerebral inoculation of the virus. Over a 4-day time course, we found a significant decrease in the weight of the VEEV TC83-inoculated  $\alpha$ Syn knockout mice (Fig. 3A). At 4 days post-infection, we analysed VEEV TC83 viral growth by plaque assay and found a significant 8.8-fold increase ( $\alpha$ Syn knockout titre  $2.27 \times 10^6 \pm 1.19 \times 10^6$  pfu/mg, wild-type titre  $2.48 \times 10^5 \pm 1.24 \times 10^5$  pfu/mg,  $P < 0.05$ ) in viral titre in the brains of  $\alpha$ Syn knockout mice compared to wild-type mice (Fig. 3B). These data indicate that VEEV TC83 exhibits increased viral growth in brain tissue of  $\alpha$ Syn knockout mice independent of interactions with the blood–brain barrier, and that  $\alpha$ Syn functions within brain tissue separate from any peripheral immune response.

Because VEEV TC83 growth was restricted within the neuronal brain tissue, we next evaluated the basal expression of type 1 interferon receptor (IFNR) in brain tissue of  $\alpha$ Syn knockout to ensure that differences in viral growth and ISG expression were not due to loss of IFNR expression. IFNR knockout mice were used as a negative control for brain tissue. Using brain tissue from mock-inoculated wild-type  $\alpha$ Syn knockout and IFNR knockout mice, we used immune fluorescence on three to four mice per group to determine IFNR expression. We found that both wild-type and  $\alpha$ Syn knockout brain tissue exhibit high levels of IFNR compared to background signal found in IFNR knockout mice (Supplementary Fig. 2, ANOVA,  $^*P = 0.0001$ ). These data show that knockout of  $\alpha$ Syn has no clear effect on IFNR expression in the brain.

Next, we determined whether  $\alpha$ Syn-dependent microglia activation was contributing to the observed differences in virus infection. Previous studies have shown that neuronal  $\alpha$ Syn expression can activate microglia and promote an inflammatory response.<sup>24–26</sup> Other studies indicate  $\alpha$ Syn-dependent activation of microglia occurs through a toll-like receptor (TLR)-dependent mechanism.<sup>25,27–31</sup> First, we evaluated the role of VEEV TC83 virus infection in activation of microglia in wild-type and  $\alpha$ Syn knockout mice. We have previously shown that VEEV TC83 infects the neurons of the CNS in  $\alpha$ Syn knockout mice but not in wild-type mice following peripheral inoculation.<sup>8</sup> We injected wild-type and  $\alpha$ Syn knockout mice by intracerebral inoculation with VEEV TC83 (TC83, 1000 pfu) and harvested brain tissue at 4 days post-infection, a time point prior to significant peripheral inflammatory cell infiltration. Flow cytometry analysis of brain tissue revealed significantly increased numbers of CD45+CD11b+CD68+ cells, CD45+CD11b+IL6+ cells and CD45+CD11b+TNFalpha+ following VEEV TC83 infection

in both wild-type and  $\alpha$ Syn knockout brain tissue, but we found no difference in CD45+CD11b+ cell activation when comparing wild-type and  $\alpha$ Syn knockout brain tissue (Supplementary Fig. 3). Next, we determined if microglial gene expression following VEEV TC83 infection in the brain was dependent on  $\alpha$ Syn expression. Using the same TC83 infection experimental model as above, CD11b+ cells were column isolated from brain tissue using CD11b antibody binding. Total RNA was extracted from CD11b+ brain cells and analysed by PCR array for ISG expression (Supplementary Fig. 3D). ISG expression was normalized to mock-infected, wild-type microglia (CD11b+ cells) and revealed similar increases in ISGs following VEEV TC83 infection in both wild-type and  $\alpha$ Syn knockout mice. These data show that  $\alpha$ Syn-dependent regulation of innate immune responses and ISG responses in the brain were not due to differences in microglia activation in wild-type and  $\alpha$ Syn knockout mice following virus infection.

Next, we utilized a human neuron culture model to evaluate the functional role of  $\alpha$ Syn in ISG expression in human neurons.<sup>13,32</sup> Wild-type and  $\alpha$ Syn knockout hESCs were differentiated into human dopaminergic neurons as previously described.<sup>13</sup> Immunofluorescence microscopy for beta-III tubulin and tyrosine hydroxylase of differentiated wild-type and  $\alpha$ Syn knockout neurons indicated they have similar neuronal morphology and dopaminergic phenotype (Fig. 3C). We infected  $\alpha$ Syn knockout and wild-type human dopaminergic neurons with VEEV TC83 virus at a MOI of 1 and determined viral titre in the supernatant at 0, 12, 24, 48 and 72 h. We found a 2-fold increase in viral titre in the  $\alpha$ Syn knockout neurons after 24 h (Fig. 3D). By 72 h,  $\alpha$ Syn knockout neurons exhibited a 19.9-fold increase in viral titre compared to wild-type neurons ( $\alpha$ Syn knockout titre  $2.20 \times 10^7 \pm 1.49 \times 10^7$  pfu/ml, wild-type titre  $1.11 \times 10^6 \pm 1.05 \times 10^6$  pfu/ml,  $P < 0.05$ ; Fig. 3D). These data show that  $\alpha$ Syn expression inhibits viral growth in neurons independent of other CNS cell types. These data and our gene expression data from  $\alpha$ Syn knockout mouse models suggested a cell autonomous role for  $\alpha$ Syn in regulating interferon responses within neurons.

### Alpha-synuclein modulates type 1 interferon responses in neurons

To evaluate our hypothesis that  $\alpha$ Syn expression supports innate immune responses within neurons, we treated  $\alpha$ Syn knockout and wild-type dopaminergic neurons with VEEV TC83 (MOI 10), poly I:C (25  $\mu$ g/ml), and T1IFN (IFN-alpha2,1000 IU/ml). We measured the expression level of IFIT1 in all three conditions due to its importance in regulating VEEV TC83 infection, and the expression level of Trim25 because it was decreased in WNV-infected  $\alpha$ Syn knockout mouse brain tissue compared to WNV-infected wild-type mice. We found that IFIT1 expression was significantly decreased by 4.8-fold in VEEV TC83-infected  $\alpha$ Syn knockout neurons compared to wild-type neurons ( $P < 0.0001$ , ANOVA with Tukey's multiple comparisons; Fig. 4A). In poly I:C-treated dopaminergic neurons, we also found a significant 11.7-fold decrease in IFIT1 expression in  $\alpha$ Syn knockout neurons compared to wild-type neurons ( $P = 0.006$ , ANOVA with Tukey's multiple comparisons; Fig. 4B). Following T1IFN treatment of dopaminergic neurons, we found a smaller but significant 1.4-fold decrease in IFIT1 expression in  $\alpha$ Syn knockout neurons compared to wild-type neurons ( $P < 0.0001$ , ANOVA with Tukey's multiple comparisons; Fig. 4C).

Next, we evaluated TRIM25 expression in  $\alpha$ Syn knockout and wild-type dopaminergic neurons and found no significant changes in TRIM25 gene expression following VEEV TC83 infection and poly I:C treatment (Fig. 4D and E). However, following treatment with

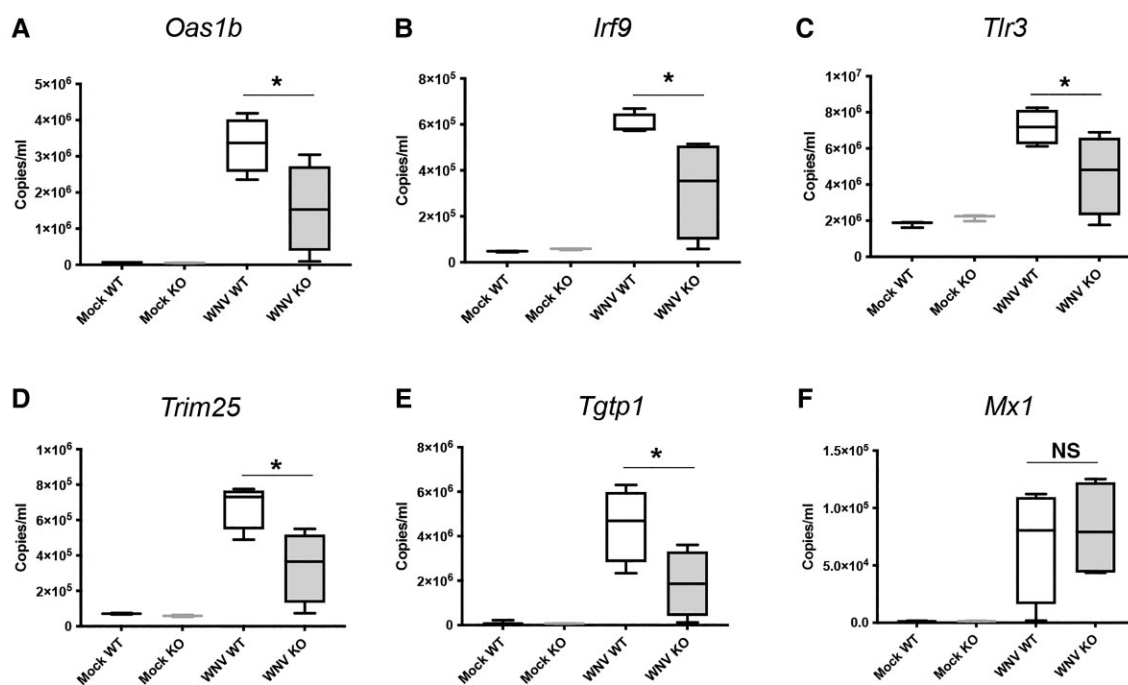


**Figure 2**  $\alpha$ Syn knockout mice exhibit decreased expression of select ISGs in the brain following WNV infection. Quantitative PCR values from brain tissue are shown in indicated treatment groups to quantify expression of ISGs identified in RNAseq analysis including: (A) *Oas1b*, (B) *Irf9*, (C) *Tlr3*, (D) *Trim25* and (E) *Tgtp1*. (F) Quantitative PCR values for *Mx1* in brain tissue of mice as an example of an ISG in the brain not altered by  $\alpha$ Syn expression.  $n = 3$  mice per treatment group. WT = wild-type mice; KO =  $\alpha$ Syn knockout mice. \* $P < 0.005$ , two-way ANOVA.

T1IFN, we found that  $\alpha$ Syn knockout neurons exhibited an 11.6-fold decrease in TRIM25 expression compared to wild-type neurons ( $P = 0.005$ , ANOVA with Tukey's multiple comparisons; Fig. 4F). These data suggest that  $\alpha$ Syn-dependent modulation of ISG responses may be occurring at the level of T1IFN signalling as *IFIT1* and *TRIM25* expression were both decreased in  $\alpha$ Syn knockout neurons following T1IFN treatment.

To evaluate the role of  $\alpha$ Syn in T1IFN signalling, we next treated  $\alpha$ Syn knockout and wild-type human dopaminergic neurons with T1IFN (10 000 IU/ml) and collected RNA from cells at 4 h post-treatment. ISG expression analysis was performed using a RT<sup>2</sup> Profiler PCR array that measures the expression level of 91 genes associated with the T1IFN signalling. We compared the expression level of these genes between IFN-treated wild-type and  $\alpha$ Syn knockout cells, using a mock treatment of wild-type cells as a control. We found that expression of most ISGs in the panel was significantly decreased in the IFN-treated  $\alpha$ Syn knockout neurons compared to wild-type neurons (Fig. 5A). In total, 61 of the assayed genes had significantly lower expression levels in  $\alpha$ Syn knockout neurons, including important mediators of the T1IFN pathway such as *STAT1* and *IRF9*, and important innate immune genes including *IFIT1*, *TLR3* and *IFNAR2* (Fig. 5B). Of note, several genes critical to the innate immune response in the brain (*IFNAR1*, *IRF9*, *JAK1*, *IL6* and *OAS2*) were among the most sensitive to loss of  $\alpha$ Syn expression with over 100-fold lower gene expression in  $\alpha$ Syn knockout neurons (Supplementary Table 2). These data indicate that  $\alpha$ Syn expression is critically important for T1IFN-dependent gene expression in neurons.

### Alpha-synuclein supports type 1 interferon signalling in neurons

Having established that  $\alpha$ Syn supports T1IFN-dependent gene expression, we sought to define the mechanisms linking  $\alpha$ Syn to interferon

signalling. We first determined whether interferon induced changes in  $\alpha$ Syn localization within human neurons. RC17 hESCs were differentiated into cortical neurons and verified to exhibit cortical neuronal markers using immunostaining for *Tbr1* and *Ctip2* at Day 55 (Supplementary Fig. 4). Cortical neurons were treated with type 1 interferon A2 (IFNa2, 10 000 IU/ml), interferon-beta (IFNB, 10 000 IU/ml) or with a media-only control for 4 h. Cortical neurons were fixed and immunostained using primary antibodies to total  $\alpha$ Syn and beta-III tubulin (TUJ1). We found that cortical neurons treated with IFNa2 exhibited significantly increased per cent of nuclei exhibiting increased total  $\alpha$ Syn (\*\* $P = 0.0004$ , control mean 4.5% versus IFNa2 17.47%, mean difference  $12.95 \pm 2.98$  SEM) and increased total  $\alpha$ Syn MFI in the nucleus (\*\*\*\* $P < 0.0001$ , control mean 3042 versus IFNa2 4048, mean difference  $1005 \pm 120.6$  SEM) compared to control treated cortical neurons (Fig. 6A, B and D;  $n = 10$  per group, unpaired t-test). Similarly, we found that cortical neurons treated with IFNB exhibited significantly increased per cent of nuclei exhibiting increased total  $\alpha$ Syn (\*\* $P = 0.0052$ , control mean 10.17% versus IFNB 19.09%, mean difference  $8.9 \pm 3.05$  SEM) and increased total  $\alpha$ Syn MFI in the nucleus (\*\*\*\* $P < 0.0001$ , control mean 2597 versus IFNB 3360, mean difference  $763 \pm 66.3$  SEM) compared to control treated cortical neurons (Fig. 6A, C and E;  $n = 10$  per group, unpaired t-test).

Because interferon treatment induced nuclear localization of  $\alpha$ Syn in neurons, we next determined the interactions between  $\alpha$ Syn and T1IFN signalling proteins over a time course. *STAT2* is phosphorylated upon T1IFN stimulation at the interferon receptor resulting in formation of a heterotrimer with phospho-*STAT1* (P-*STAT1*) and *IRF9*, which translocates to the nucleus.<sup>33</sup> Because of the large number of neurons needed for these studies, we utilized primary murine cortical neurons as previously described.<sup>16</sup> Primary murine cortical neurons were treated with mock control (PBS) or IFNa2 and harvested for immune fluorescence analysis at 1 and 4 h post-treatment. At both 1 and 4 h after IFNa2 treatment,  $\alpha$ Syn in cortical neurons exhibited significantly



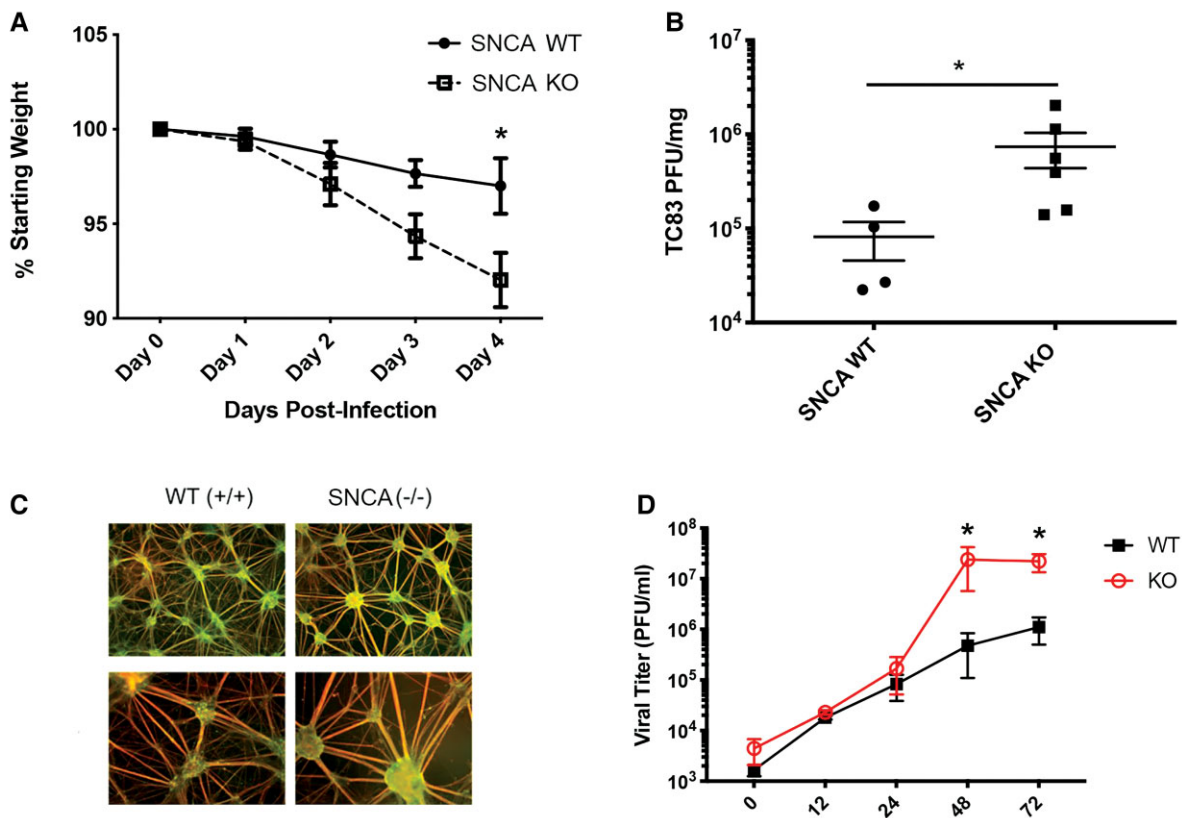


**Figure 3**  $\alpha$ Syn expression restricts VEEV TC83 infection in murine brain tissue and human dopaminergic neurons. Wild-type (WT) and  $\alpha$ Syn knockout (KO) mice were inoculated with VEEV TC83 ( $10^5$  pfu, intracerebral inoculation) and (A) followed for weight loss over the indicated time period.  $n = 6$  mice per group.  $*P < 0.0001$ , two-way ANOVA. (B) At 4 days post-infection with VEEV TC83, brain tissue was analysed for VEEV TC83 viral titre using plaque assay.  $n = 4$ –6 mice per group.  $*P = 0.038$ , Mann–Whitney U-test. (C) Wild-type and  $\alpha$ Syn knockout human dopaminergic neurons, differentiated for 42 days, were positive for beta-III tubulin (CY3, red) and tyrosine hydroxylase (FITC, green). (D) Wild-type and  $\alpha$ Syn knockout neurons were inoculated with VEEV TC83 (MOI 1) and supernatant collected at indicated time points for viral titre assay.  $*P < 0.05$ , two-way ANOVA.  $n = 4$  replicates per group. Images shown at 63 $\times$  original magnification.

increased co-localized signal with phosphorylated-Stat2(Tyr690) (Fig. 7A–D,  $n = 3$  experiments and 12–17 images per group, ANOVA of Manders 2 signal co-localization with Costes  $P = 1$ ,  $*P < 0.0001$ , Tukey's multiple comparisons test).

To investigate  $\alpha$ Syn and STAT2 interactions in human dopaminergic neurons, wild-type and  $\alpha$ Syn knockout human dopaminergic neurons were plated and differentiated for 42 days. We treated the neurons with IFN $\alpha$ 2 (10 000 IU/ml) or PBS vehicle control for 4 h and determined protein expression of phospho-STAT2 (pSTAT2) and total STAT2 using enzyme-linked immunosorbent assay (ELISA). We found that human dopaminergic  $\alpha$ Syn knockout neurons exhibit significantly decreased pSTAT2 expression compared to wild-type neurons with no effect on total STAT2 expression (Fig. 7E–F,  $n = 5$  per group in two experimental replicates, ANOVA,  $*P = 0.0251$ ).

Because  $\alpha$ Syn exhibited evidence of co-localization and regulation of pSTAT2 expression, we next evaluated  $\alpha$ Syn co-localization with phosphorylated STAT1 (pSTAT1) and IFN $\alpha$ 2 in murine cortical neurons as described above. Primary murine cortical neurons were treated with mock control (PBS) or IFN $\alpha$ 2 and harvested for immune fluorescence analysis at 1 and 4 h post-treatment as above. We found that  $\alpha$ Syn co-localized with pSTAT1(Tyr701) at 1 h post-treatment but not at 4 h post-treatment (Supplementary Fig. 5,  $n = 15$ –20 per group in three experimental replicates, one-way ANOVA with multiple comparisons test of Manders 2 values with Costes  $P = 1$ ,  $*P < 0.0001$ ). Subsequent analysis of  $\alpha$ Syn co-

localization with the IFN $\alpha$ 2 in interferon-treated mouse cortical neurons revealed no evidence of changes in co-localization between the two signals following IFN $\alpha$ 2 treatment (Supplementary Fig. 6).

### Viral infection induces phosphorylation of alpha-synuclein

Because our studies had evaluated total  $\alpha$ Syn expression in murine brain tissue and human neurons, we next investigated whether phosphorylation at the S129 position in  $\alpha$ Syn (pS129  $\alpha$ Syn) was associated with viral infection in human brain tissue. A prior study showed that infection with an alphavirus in mice resulted in increased expression of pS129  $\alpha$ Syn in brain tissue,<sup>12</sup> and T1IFN responses are an important primary innate immune response and critical to limiting virus-induced cell death in brain tissue.<sup>34,35</sup> pS129 $\alpha$ Syn is also commonly found in Lewy bodies in Parkinson's disease and is a hallmark characteristic of the condition,<sup>36</sup> but the expression pattern and levels of pS129  $\alpha$ Syn is not known in human cases of viral encephalitis. We obtained sections from subcortical brain tissue from five patients with a pathological and clinical diagnosis of WNV encephalitis and four control patients and evaluated expression of total and pS129  $\alpha$ Syn in human brain tissue (Supplementary Table 3). We completed immunofluorescence imaging analysis for pS129  $\alpha$ Syn expression in subcortical and cortical grey matter from control patients and subcortical grey matter from



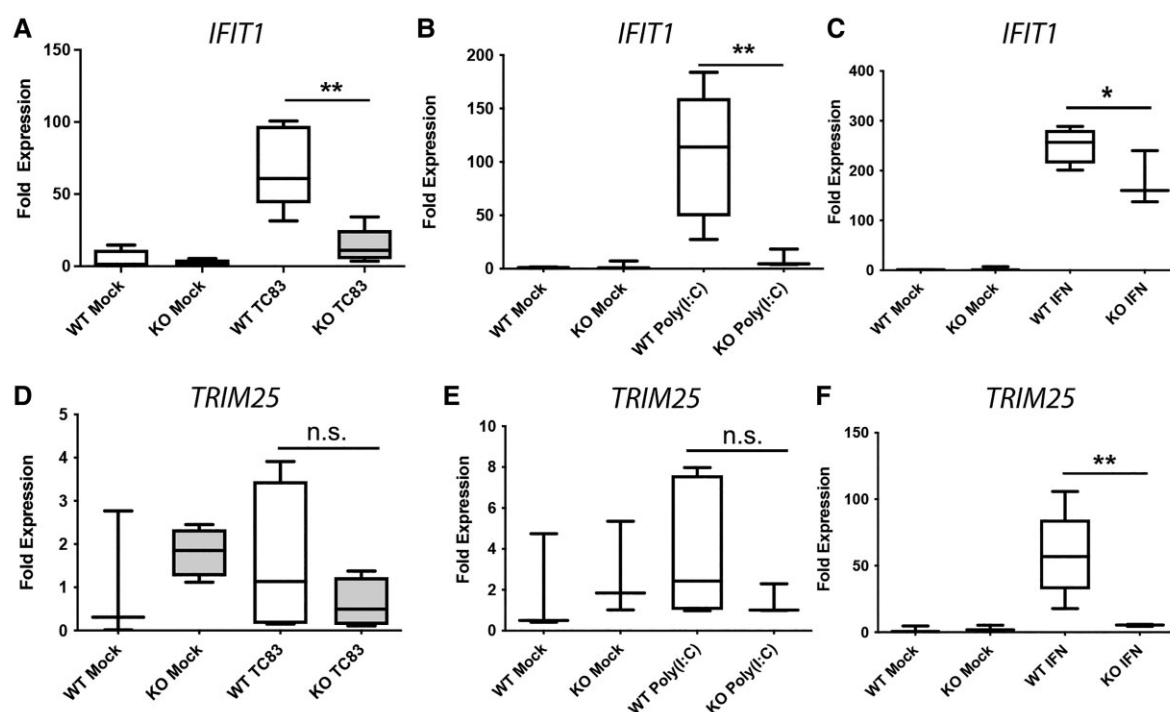


**Figure 4**  $\alpha$ Syn expression supports IFIT1 and TRIM25 gene expression in human neurons. Wild-type (WT) and  $\alpha$ Syn knockout (KO) neurons were inoculated with mock or VEEV TC83 (MOI 10) and neurons were harvested at 12 h post-infection for gene expression analysis. (A) Following VEEV TC83 infection, IFIT1 gene expression increased 17-fold in wild-type neurons and 6-fold in  $\alpha$ Syn knockout neurons. \*\* $P < 0.01$ . (B) Poly I:C (25  $\mu$ g/ml) induced IFIT1 expression 100-fold in wild-type neurons and 3-fold in  $\alpha$ Syn knockout neurons. \*\* $P < 0.01$ . (C) Following T1IFN treatment (10 000 IU/ml), IFIT1 gene expression was significantly reduced in  $\alpha$ Syn knockout neurons compared to wild-type neurons.  $n = 3-5$  per group. \* $P < 0.05$ , ANOVA with Tukey's multiple comparisons. (D and E) TRIM25 gene expression was not significantly increased following VEEV TC83 infection or poly I:C treatment.  $n = 4-5$  replicates per group. (F) Wild-type and  $\alpha$ Syn knockout neurons were treated with T1IFN (1000 IU/ml) and cells harvested at 4 h post-treatment for qPCR analysis. TRIM25 gene expression increased 32-fold in wild-type neurons with T1IFN treatment and 1.9-fold in  $\alpha$ Syn knockout neurons. \*\* $P < 0.05$ , ANOVA, Tukey's multiple comparisons.  $n = 3-5$  per group.

WNV-infected (Fig. 8B) patients. Using grader-blinded scoring for MFI in images from each patient, we found that pS129  $\alpha$ Syn expression is significantly increased by 5-fold in WNV-infected subcortical grey matter (mean MFI = 651253,  $n = 5$ ) compared to control brain tissue (mean MFI = 651253, 95% CI, 262404, 789881; Fig. 8C, control tissue  $n = 4$  patients,  $P = 0.0022$ ). To evaluate for cell-type localization of pS129  $\alpha$ Syn in human brain tissue, we next evaluated human brain tissue for co-localization between pS129  $\alpha$ Syn and a neuron marker (MAP2). We found that pS129  $\alpha$ Syn expression in WNV-infected brain tissue co-localized with the neuron marker MAP2 (Fig. 8D and E). These data show for the first time that viral infection in humans leads to increased expression of phosphorylated S129  $\alpha$ Syn in neurons.

## Discussion

$\alpha$ Syn is a highly conserved protein expressed in neurons of most vertebrate species. Its unique localization to nuclei as well as synaptic puncta suggests it may have functions beyond synaptic biology. Mounting evidence supports an important role for  $\alpha$ Syn in protection of neurons, but the mechanisms of protection remain unclear.<sup>8,11,12</sup> Our data show that during virus infection,  $\alpha$ Syn supports expression of ISGs required to inhibit viral infection. This was confirmed both *in vivo* in murine infection models and in a human neuronal culture system. Moreover, the same ISGs stimulated by virus infection are also dependent on  $\alpha$ Syn for expression following poly I:C and T1IFN treatment. The importance of  $\alpha$ Syn-dependent ISG expression is supported by our

findings showing that VEEV TC83 growth is significantly increased in  $\alpha$ Syn knockout neurons and in  $\alpha$ Syn knockout brain tissue compared to wild-type neurons and mice, respectively. VEEV TC83 is attenuated due to a mutation in a 5' untranslated region that results in increased IFIT1 restriction of viral growth,<sup>37</sup> and our discovery of increased viral growth in the absence of  $\alpha$ Syn expression suggested that IFIT1 protein activity was decreased in  $\alpha$ Syn knockout neurons. We subsequently found evidence of decreased IFIT1 expression in  $\alpha$ Syn knockout neurons following VEEV TC83 infection and following treatment with poly I:C. These data show that  $\alpha$ Syn expression supports ISG responses that are critical to control RNA virus infection in neurons.

We also show that VEEV TC83 infection and poly I:C treatment did not significantly increase expression of TRIM25 in wild-type human neurons, while treatment with IFN $\alpha$ 2 resulted in significantly increased expression of TRIM25. In human  $\alpha$ Syn knockout neurons, expression of TRIM25 was significantly decreased compared to wild-type neurons following treatment with T1IFN. As  $\alpha$ Syn-dependent expression of TRIM25 occurs downstream of T1IFN stimulation but not poly I:C stimulation in our neuron model, we hypothesized that  $\alpha$ Syn interacts with T1IFN signalling pathways to support and regulate ISG expression in neurons. We investigated this by measuring the expression of several key components of the interferon and STAT signalling pathways following T1IFN treatment of neurons. Using a PCR array for ISG expression, we found a broad decrease in ISG expression in  $\alpha$ Syn knockout human neurons following T1IFN stimulation. This

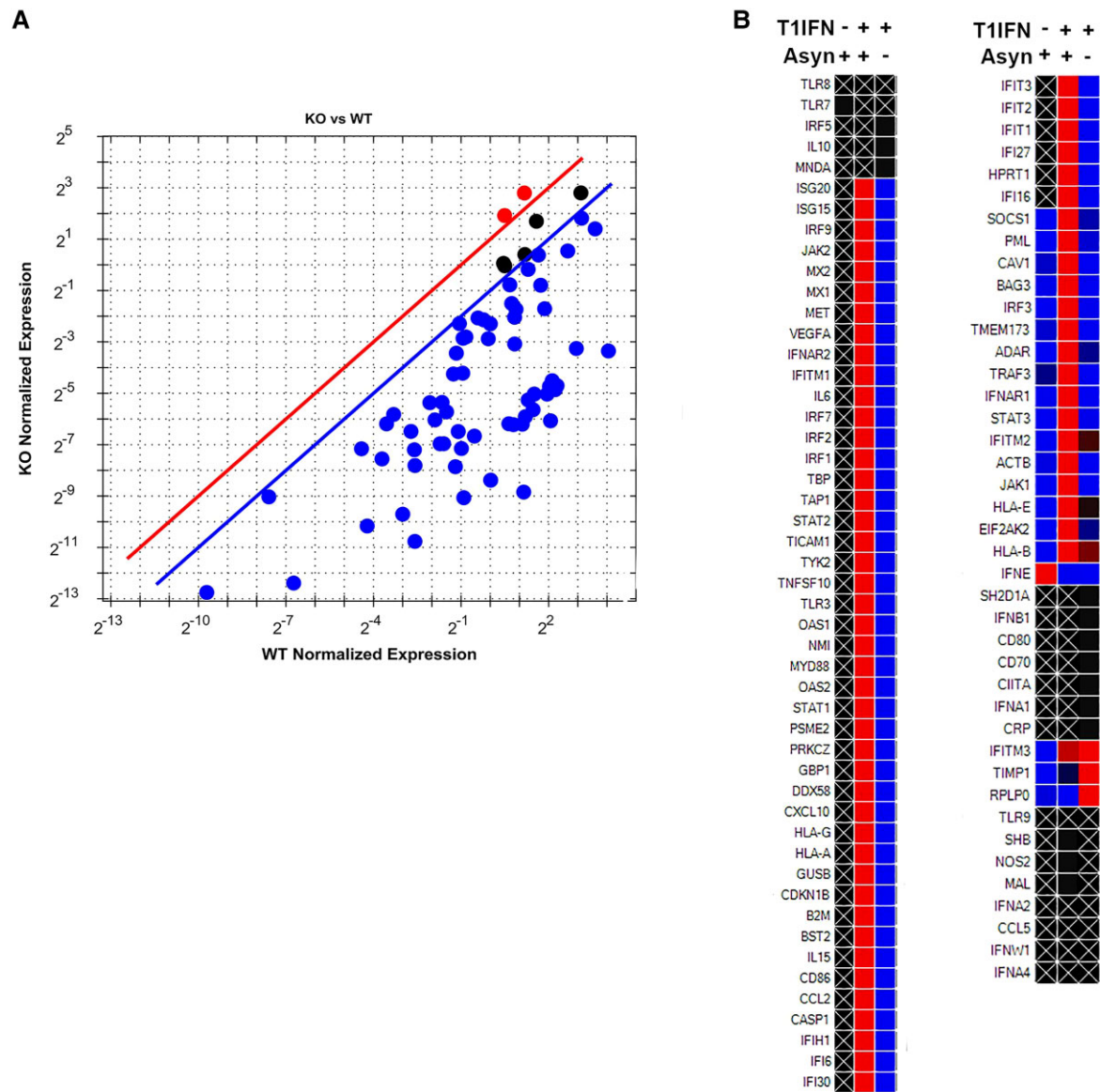


**Figure 5**  $\alpha$ Syn expression supports T1IFN-dependent ISG expression in human dopaminergic neurons. Wild-type (WT) and  $\alpha$ Syn knockout (KO) neurons were treated with T1IFN (10 000 IU/ml) and cells harvested at 4 h post-treatment for analysis using ISG expression PCR array. (A) Graphic representation of ISG relative gene expression comparing  $\alpha$ Syn knockout neurons (y-axis) to wild-type neurons (x-axis). (B) Heat map of ISGs showing relative gene expression compared to control-treated wild-type neurons in individual treatment groups. Blue = decreased expression; black = no change; red = increased expression.

finding provides insight into the mechanism by which mice and neurons lacking  $\alpha$ Syn expression are deficient in combating viral growth because T1IFN-dependent expression of ISGs are a primary mechanism of immune restriction in the CNS.<sup>38</sup>

We next investigated the mechanism by which  $\alpha$ Syn expression alters ISG expression. Following type I IFN treatment of  $\alpha$ Syn knockout and  $\alpha$ Syn wild-type human neurons, our data show that  $\alpha$ Syn co-localizes with phosphorylated STAT2, and we found reduced levels of pSTAT2 protein when  $\alpha$ Syn expression was knocked out of human neurons. These data suggest that  $\alpha$ Syn localizes with pSTAT2 following interferon stimulation and supports activation. Interestingly, we also found that pSTAT1 co-localized with  $\alpha$ Syn at 1 h post-treatment, and that  $\alpha$ Syn localizes to the nucleus following IFN $\alpha$ 2 and IFN $\beta$  treatment. Previous studies have reported the nuclear translocation of  $\alpha$ Syn under conditions of oxidative stress<sup>39</sup>

and exposure to toxins, such as paraquat.<sup>40</sup> However,  $\alpha$ Syn nuclear localization has not been described in response to a signal transduction pathway, such as the IFN pathway. This is the first report that  $\alpha$ Syn is translocating to the nucleus in association with STAT activation to support ISG expression in neurons. To confirm links between  $\alpha$ Syn and immune responses in human brain tissue, we investigated the expression of phosphorylated S129  $\alpha$ Syn in virus-infected human brain tissue. Previous studies had shown that pS129  $\alpha$ Syn was increased in the mouse brain following alphavirus infection.<sup>12</sup> In our studies, we found that pS129  $\alpha$ Syn levels increase in human brain tissue following WNV infection, and that pS129  $\alpha$ Syn localized with neurons in human brain tissue.

These data confirmed our findings that  $\alpha$ Syn responds to infection and inflammatory pathways and suggest that pS129  $\alpha$ Syn may have a functional role following virus infection. The specific interactions of

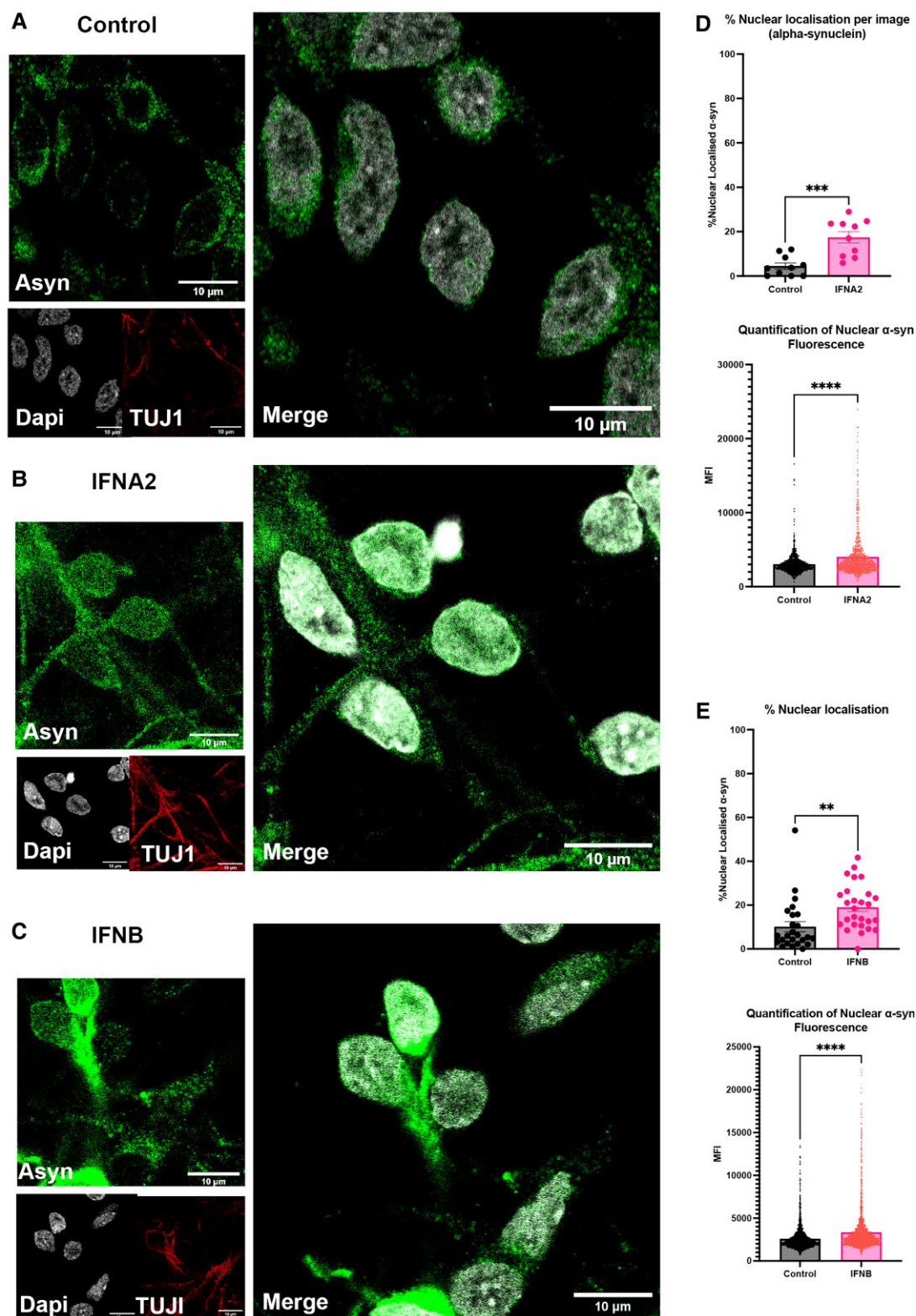


**Figure 6** αSyn localizes to the nucleus following T1IFN stimulation. Human cortical neurons were treated with (A) media control, (B) interferon-alpha2 (IFNα2, 10 000 IU/ml) or (C) interferon-beta (IFNβ, 10 000 IU/ml). At 4 h post-treatment, neurons were analysed for expression total αSyn (Asyn, FITC/green), a neuron marker (TUJ1, CY3/red) and DAPI (white). (D) The percent of cortical neurons expressing αSyn in the nucleus per image was determined (\*\*\* $P=0.0004$ , control mean 4.5% versus IFNα2 17.47%, mean difference  $12.95 \pm 2.98$  SEM) and total αSyn MFI in the nucleus was determined (\*\*\*\* $P<0.0001$ , control mean 3042 versus IFNα2 4048, mean difference  $1005 \pm 120.6$  SEM,  $n=10$  per group, unpaired t-test). (E) Cortical neurons treated with IFNβ were analysed for per cent of nuclei exhibiting increased total αSyn (\*\* $P=0.0052$ , control mean 10.17% versus IFNβ 19.09%, mean difference  $8.9 \pm 3.05$  SEM) and αSyn MFI in the nucleus (\*\*\*\* $P<0.0001$ , control mean 2597 versus IFNβ 3360, mean difference  $763 \pm 66.3$  SEM). Scale bar = 10 μm, images shown at 63× original magnification.



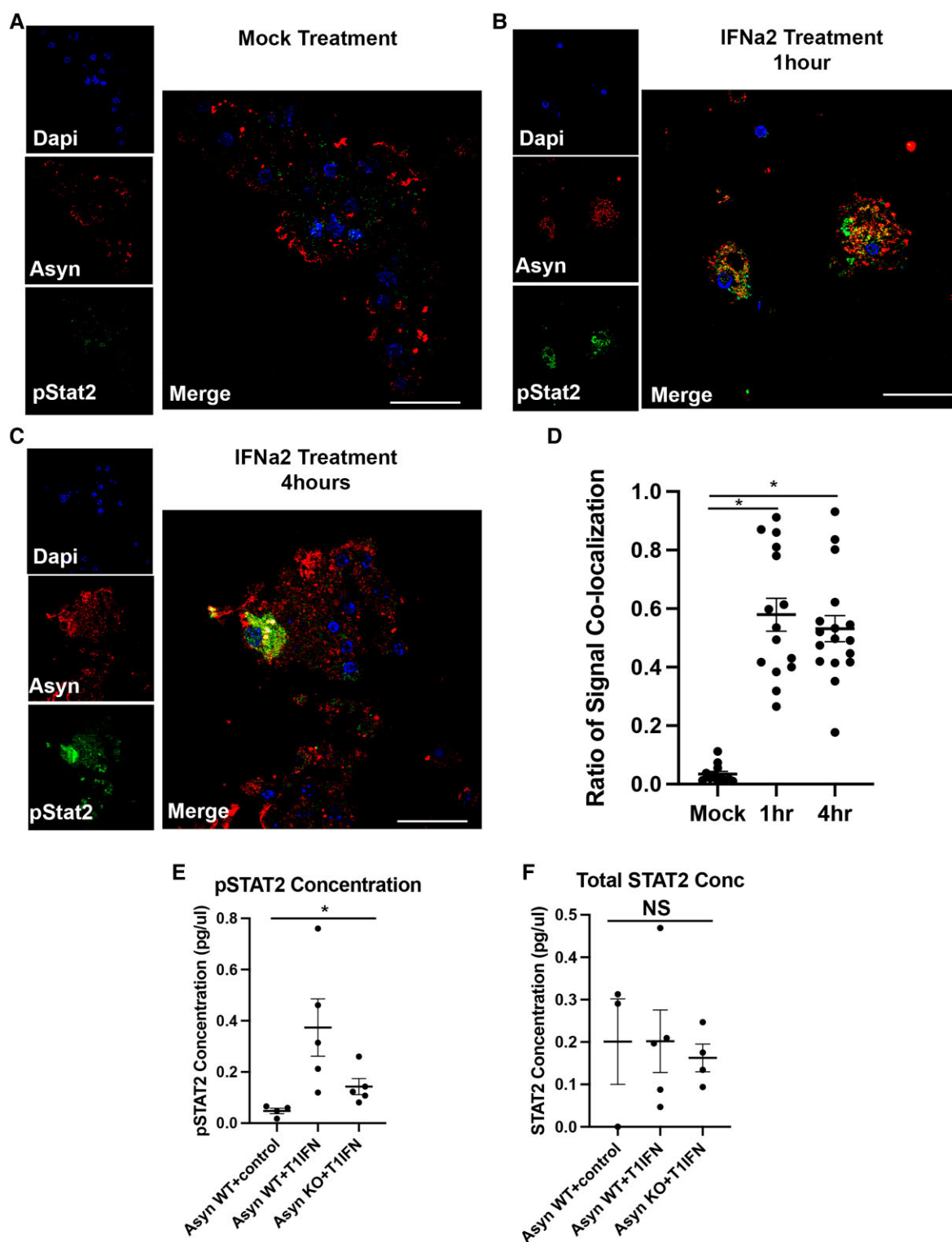


**Figure 7** αSyn localizes with pSTAT2 and supports pSTAT2 expression in neurons. Mouse cortical neurons were treated with (A) control or T1IFN (IFNa2, 10 000 IU/ml) for (B) 1 h or (C) 4 h and labelled using immunofluorescence analysis for αSyn (Asyn) (CY5/red) and pSTAT2 (FITC/green) expression. (D) Cortical neurons were analysed for αSyn co-localization with pSTAT2 using Fiji Co-loc analysis for Manders 2 ratios of αSyn signal that co-localizes with pSTAT2 signal (\* $P < 0.0001$ ,  $n = 12$ –17 per group). (E and F) Human dopaminergic neurons expressing αSyn (WT) or knockout of αSyn (Asyn KO) were treated with IFNa2 (10 000 IU/ml) or control and harvested at 4 h post-treatment for ELISA analysis of pSTAT2 and total STAT2 expression (wild-type + control,  $n = 4$ ; wild-type + T1IFN,  $n = 5$ ; Asyn knockout + T1IFN,  $n = 5$ ;  $P < 0.05$  two-sided ANOVA). Images 60× original magnification. Scale bar = 50 μm.



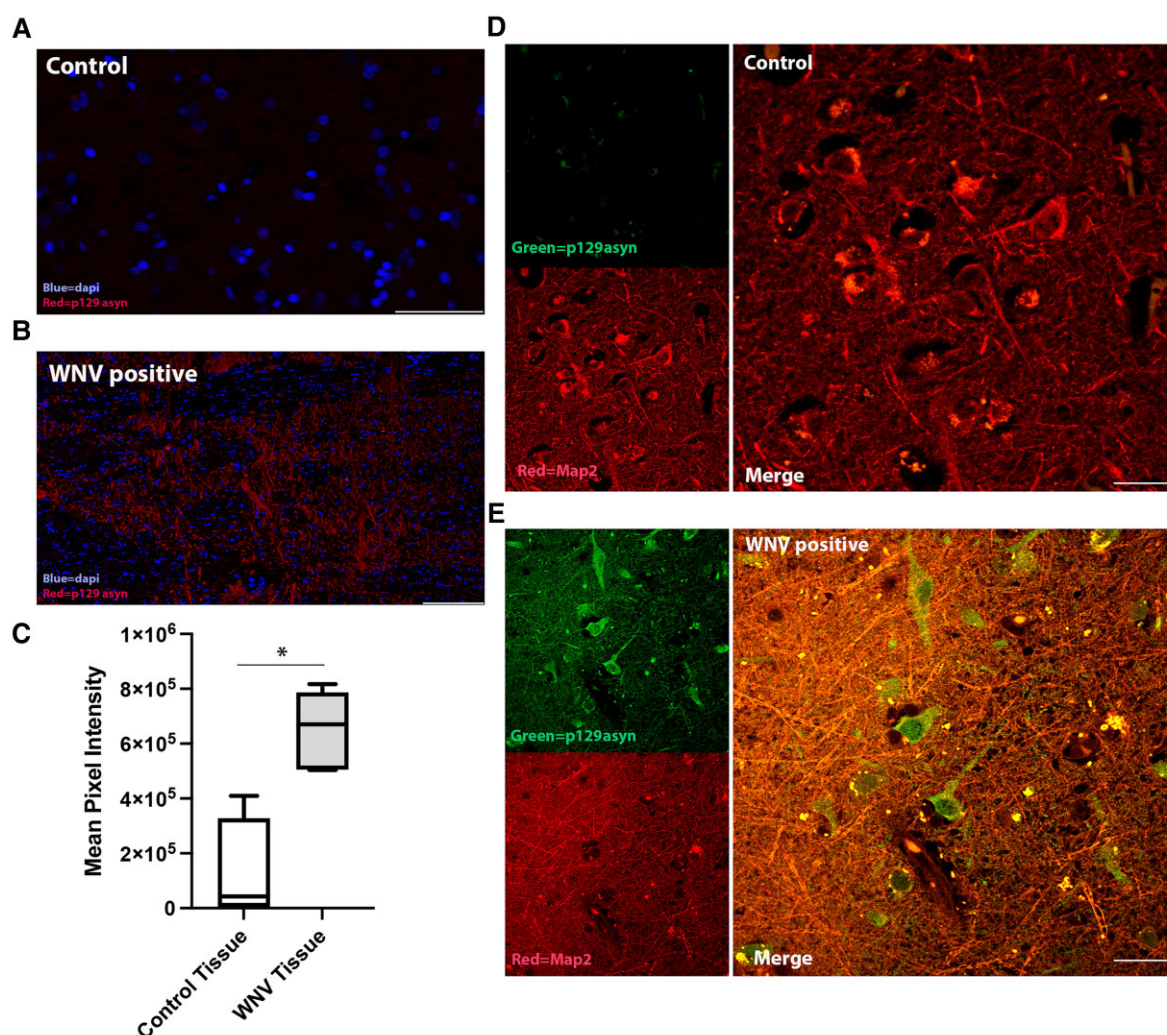


**Figure 8** Viral infection of human brain tissue results in increased expression of phospho-S129  $\alpha$ Syn. Immunofluorescent histology for phospho-S129  $\alpha$ Syn (Asyn) (CY3, red) of (A) control human brain tissue ( $n=4$ , scale bar = 50  $\mu$ M) and (B) WNV-infected human subcortical grey matter tissue ( $n=5$ , scale bar = 200  $\mu$ M). Blue = DAPI nuclear staining. Images shown at 40 $\times$  original magnification. (C) Measure of MFI units per field of phospho-S129  $\alpha$ Syn staining of human brain tissue acutely infected with WNV. Unpaired, two-tailed t-test, \* $P=0.002$ . Immunofluorescent histology images from human grey matter tissue of a representative (D) control patient and (E) a patient with WNV encephalitis. Green/FITC = pS129 Asyn, red/CY3 = MAP2. Scale bar = 50  $\mu$ M. Images shown at 60 $\times$  original magnification.

pS129  $\alpha$ Syn and related post-translational modifications in  $\alpha$ Syn are not known but are an important future direction for this work. Studies have suggested that  $\alpha$ Syn has a role in histone modification to facilitate transcription and it may regulate NF- $\kappa$ B expression in models with overexpression  $\alpha$ Syn.<sup>41,42</sup> Thus, we hypothesize that, during T1IFN stimulation in neurons,  $\alpha$ Syn interacts directly with pSTAT2 to support nuclear translocation of the pSTAT1–pSTAT2 heterodimer, and thereby directly facilitates transcription of ISGs. The role of  $\alpha$ Syn in the support of T1IFN signalling seems to be specific to fully differentiated neurons, as we have been unable to replicate these phenotypes in non-neuron cell types.

These data do not provide information on interactions between T1IFN and overexpressed or misfolded  $\alpha$ Syn. Future studies will need to evaluate these important protein interactions. Also, prior studies have shown that loss of IFNB signalling results in increased Parkinson's disease features in a murine model.<sup>43</sup> While our studies did not evaluate loss of T1IFN signalling on  $\alpha$ Syn expression and localization, these prior findings support our findings that interferon

signalling exhibits important interactions with  $\alpha$ Syn expression. Importantly, our data also provide a mechanism for our previously reported observations that mice deficient in  $\alpha$ Syn fail to control neuroinvasive viral infection. Our data also indicate that virus infection increases expression of phosphorylated S129  $\alpha$ Syn in neurons of human brain tissue. Future studies will need to determine interactions between interferon stimulation and formation of Parkinson's disease-related fibrils, oligomers or pS129  $\alpha$ Syn. Studies evaluating the interactions between interferon signalling and  $\alpha$ Syn post-translational modifications are needed to evaluate the role of  $\alpha$ Syn-dependent T1IFN signalling events in the pathogenesis of synucleinopathies like Parkinson's disease.

## Acknowledgements

The imaging experiments were performed in the Advanced Light Microscopy Core part of NeuroTechnology Center at University of

Colorado Anschutz Medical Campus supported in part by Rocky Mountain Neurological Disorders Core Grant Number P30 NS048154 and by Diabetes Research Center Grant Number P30 DK116073.

## Funding

This work was supported by VA Merit Award (I01BX003863), NIH/NINDS R01 NS123431 and NIH/NIAID R01 AI153724 to J.D.B. The contents are the authors' sole responsibility and do not necessarily represent official NIH views. Y.C., R.B. and T.K. were supported by funding from the UK Centre for Mammalian Synthetic Biology and Medical Research Council Grant: MR/K017276/1. A.C. was supported by funding from the Anne Rowling Regenerative Neurology Clinic.

## Competing interests

The authors report no competing interests.

## Supplementary material

[Supplementary material](#) is available at *Brain* online.

## References

- Spillantini MG, Goedert M. The  $\alpha$ -synucleinopathies: Parkinson's disease, dementia with Lewy bodies, and multiple system atrophy. *Ann N Y Acad Sci*. 2000;920:16–27.
- Clayton DF, George JM. The synucleins: A family of proteins involved in synaptic function, plasticity, neurodegeneration and disease. *Trends Neurosci*. 1998;21:249–254.
- Barbour R, Kling K, Anderson JP, et al. Red blood cells are the major source of alpha-synuclein in blood. *Neurodegener Dis*. 2008;5:55–59.
- Abeliovich A, Schmitz Y, Fariñas I, et al. Mice lacking  $\alpha$ -synuclein display functional deficits in the nigrostriatal dopamine system. *Neuron*. 2000;25:239–252.
- Chandra S, Fornai F, Kwon HB, et al. Double-knockout mice for  $\alpha$ - and  $\beta$ -synucleins: Effect on synaptic functions. *Proc Natl Acad Sci U S A*. 2004;101:14966–14971.
- Cabin DE, Shimazu K, Murphy D, et al. Synaptic vesicle depletion correlates with attenuated synaptic responses to prolonged repetitive stimulation in mice lacking  $\alpha$ -synuclein. *J Neurosci*. 2002;22:8797–8807.
- Burré J, Sharma M, Tsetsenis T, Buchman V, Etherton MR, Südhof TC.  $\alpha$ -Synuclein promotes SNARE-complex assembly in vivo and in vitro. *Science*. 2010;329:1663–1667.
- Beatman EL, Massey A, Shives KD, et al. Alpha-synuclein expression restricts RNA viral infections in the brain. *J Virol*. 2015;90:2767–2782.
- Stolzenberg E, Berry D, Yang D, et al. A role for neuronal alpha-synuclein in gastrointestinal immunity. *J Innate Immun*. 2017;9:456–463.
- Alam MM, Yang De, Li XQ, et al. Alpha synuclein, the culprit in Parkinson disease, is required for normal immune function. *Cell Rep*. 2022;38:110090.
- Tomlinson JJ, Shutinoski B, Dong L, et al. Holocranohistochemistry enables the visualization of  $\alpha$ -synuclein expression in the murine olfactory system and discovery of its systemic anti-microbial effects. *J Neural Trans (Vienna)*. 2017;124:721–738.
- Bantle CM, Phillips AT, Smeyne RJ, Rocha SM, Olson KE, Tjalkens RB. Infection with mosquito-borne alphavirus induces selective loss of dopaminergic neurons, neuroinflammation and widespread protein aggregation. *NPJ Parkinsons Dis*. 2019;5:20.
- Chen Y, Dolt KS, Kriek M, et al. Engineering synucleinopathy-resistant human dopaminergic neurons by CRISPR-mediated deletion of the SNCA gene. *Eur J Neurosci*. 2019;49:510–524.
- Drummond NJ, Singh Dolt K, Canham MA, Kilbride P, Morris GJ, Kunath T. Cryopreservation of human midbrain dopaminergic neural progenitor cells poised for neuronal differentiation. *Front Cell Dev Biol*. 2020;8:578907.
- Shi Y, Kirwan P, Livesey FJ. Directed differentiation of human pluripotent stem cells to cerebral cortex neurons and neural networks. *Nat Protoc*. 2012;7:1836–1846.
- Beatman E, Oyer R, Shives KD, et al. West Nile virus growth is independent of autophagy activation. *Virology*. 2012;433:262–272.
- Posel C, Moller K, Boltze J, Wagner DC, Weise G. Isolation and flow cytometric analysis of immune cells from the ischemic mouse brain. *J Vis Exp*. 2016;108:53658.
- Perfetto SP, Ambrozak D, Nguyen R, Chattopadhyay PK, Roederer M. Quality assurance for polychromatic flow cytometry using a suite of calibration beads. *Nat Protoc*. 2012;7:2067–2079.
- Cho H, Diamond MS. Immune responses to West Nile virus infection in the central nervous system. *Viruses*. 2012;4:3812–3830.
- Lim JK, Lisco A, McDermott DH, et al. Genetic variation in OAS1 is a risk factor for initial infection with West Nile virus in man. *PLoS Pathog*. 2009;5:e1000321.
- Kong KF, Delroux K, Wang X, et al. Dysregulation of TLR3 impairs the innate immune response to West Nile virus in the elderly. *J Virol*. 2008;82:7613–7623.
- Bigham AW, Buckingham KJ, Husain S, et al. Host genetic risk factors for West Nile virus infection and disease progression. *PLoS One*. 2011;6:e24745.
- Hyde JL, Gardner CL, Kimura T, et al. A viral RNA structural element alters host recognition of nonself RNA. *Science*. 2014;343:783–787.
- Harms AS, Cao S, Rowse AL, et al. MHCII Is required for alpha-synuclein-induced activation of microglia, CD4 T cell proliferation, and dopaminergic neurodegeneration. *J Neurosci*. 2013;33:9592–9600.
- Roodveldt C, Labrador-Garrido A, Gonzalez-Rey E, et al. Preconditioning of microglia by alpha-synuclein strongly affects the response induced by toll-like receptor (TLR) stimulation. *PLoS One*. 2013;8:e79160.
- Schapansky J, Nardozi JD, LaVoie MJ. The complex relationships between microglia, alpha-synuclein, and LRRK2 in Parkinson's disease. *Neuroscience*. 2015;302:74–88.
- Beraud D, Hathaway HA, Trecki J, et al. Microglial activation and antioxidant responses induced by the Parkinson's disease protein alpha-synuclein. *J Neuroimmune Pharmacol*. 2013;8:94–117.
- Beraud D, Twomey M, Bloom B, et al.  $\alpha$ -Synuclein alters toll-like receptor expression. *Front Neurosci*. 2011;5:80.
- Caplan IF, Maguire-Zeiss KA. Toll-like receptor 2 signaling and current approaches for therapeutic modulation in synucleinopathies. *Front Pharmacol*. 2018;9:417.
- Roodveldt C, Labrador-Garrido A, Gonzalez-Rey E, et al. Glial innate immunity generated by non-aggregated alpha-synuclein in mouse: Differences between wild-type and Parkinson's disease-linked mutants. *PLoS One*. 2010;5:e13481.
- Sanchez-Guajardo V, Tentillier N, Romero-Ramos M. The relation between alpha-synuclein and microglia in Parkinson's disease: Recent developments. *Neuroscience*. 2015;302:47–58.
- Petersen K, Olesen OF, Mikkelsen JD. Developmental expression of  $\alpha$ -synuclein in rat hippocampus and cerebral cortex. *Neuroscience*. 1999;91:651–659.

33. Greenlund AC, Morales MO, Viviano BL, Yan H, Krolewski J, Schreiber RD. Stat recruitment by tyrosine-phosphorylated cytokine receptors: An ordered reversible affinity-driven process. *Immunity*. 1995;2:677–687.
34. Grubaugh ND, Massey A, Shives KD, Stenglein MD, Ebel GD, Beckham JD. West Nile virus population structure, injury, and interferon-stimulated gene expression in the brain from a fatal case of encephalitis. *Open Forum Infect Dis*. 2015;3: ofv182.
35. Lesteberg KE, Beckham JD. Immunology of West Nile virus infection and the role of alpha-synuclein as a viral restriction factor. *Viral Immunol*. 2019;32:38–47.
36. Fujiwara H, Hasegawa M, Dohmae N, et al.  $\alpha$ -Synuclein is phosphorylated in synucleinopathy lesions. *Nat Cell Biol*. 2002;4:160–164.
37. Reynaud JM, Kim DY, Atasheva S, et al. IFIT1 differentially interferes with translation and replication of alphavirus genomes and promotes induction of type I interferon. *PLoS Pathog*. 2015; 11:e1004863.
38. Lobigs M, Müllbacher A, Wang Y, Pavy M, Lee E. Role of type I and type II interferon responses in recovery from infection with an encephalitic flavivirus. *J Gen Virol*. 2003;84:567–572.
39. Xu S, Zhou M, Yu S, et al. Oxidative stress induces nuclear translocation of C-terminus of  $\alpha$ -synuclein in dopaminergic cells. *Biochem Biophys Res Commun*. 2006;342:330–335.
40. Goers J, Manning-Bog AB, McCormack AL, et al. Nuclear localization of  $\alpha$ -synuclein and its interaction with histones. *Biochemistry*. 2003;42:8465–8471.
41. Lee JY, Kim H, Jo A, et al.  $\alpha$ -Synuclein A53T binds to transcriptional adapter 2-alpha and blocks histone H3 acetylation. *Int J Mol Sci*. 2021;22:5392.
42. Yuan Y, Jin J, Yang B, et al. Overexpressed alpha-synuclein regulated the nuclear factor-kappaB signal pathway. *Cell Mol Neurobiol*. 2008;28:21–33.
43. Ejlerskov P, Hultberg JG, Wang J, et al. Lack of neuronal IFN-beta-IFNAR causes Lewy body- and Parkinson's disease-like dementia. *Cell*. 2015;163:324–339.